Record Charging Events from Applied Technology Satellite 6

R. C. Olsen*
University of Alabama, Huntsville, Alabama

Applied Technology Satellite 6 regularly charged to large negative potentials in sunlight and eclipse in the Earth's midnight to dawn region. This geosynchronous satellite normally reached potentials of −100 to −1000 V in sunlight, and potentials of −100 to −10,000 V in eclipse. The largest potential recorded in eclipse for this satellite was −19 kV, in an environment characterized by an electron temperature of 18 keV. The most negative potential recorded in sunlight was −2 kV, at local dawn, while immersed in an 11-keV electron population. These are the most negative potentials reported from the geosynchronous orbit to date for eclipse and sunlight, respectively. The magnitudes of these potentials indicate the need for methods of potential control on satellites at these altitudes, particularly those with shadowed insulating surfaces.

Introduction

REPORTS of large negative potentials on satellites in geosynchronous orbit began with Applied Technology Satellite 5 (ATS-5), launched in 1969.[1] This satellite regularly charged to several kilovolts in eclipse if there had been magnetic activity (substorms) in the hours prior to or during eclipse. Somewhat more rarely, the satellite charged negatively in sunlight reaching potentials of −50 to −300 V.[2] Daylight charging was normally accompanied by charging signatures indicating differential potentials on the spacecraft surface of hundreds of volts.[3]

The charging phenomena on ATS-5 were eclipsed by the larger measurements found on Applied Technology Satellite 6 (ATS-6), launched in 1974. ATS-6 charged negatively in eclipse, often to many kilovolts.[4,5] Like ATS-5 in sunlight, it was found that ATS-6 regularly charged hundreds of volts negative in sunlight, up to 50% of the time in the midnight-to-dawn region.[6] It was shown that there was also a substantial level of differential charging on the spacecraft surface, with differential potentials of hundreds of volts inferred from the particle data.[7] ATS-5 and ATS-6 reached similar potentials when in the same eclipse-charging environment. The differences in daylight charging occurrence frequency and magnitude have been ascribed to the effects of spin rate, geometry and materials, and the processes associated with differential charging.[3] (ATS-5 spun at 100 rpm, ATS-6 was three-axis-stabilized.)

In this paper, the largest (most negative) charging events for ATS-6 in eclipse and sunlight are shown. After several years of study of ATS-5, ATS-6, and SCATHA data, it is believed that these are the most negative potentials ever measured at geosynchronous orbit. Our purpose for presenting these events is to document them properly, and clearly demonstrate the magnitudes which satellite potentials have been observed to reach. In contrast to recent articles defining "worst-case" charging environments,[8,9] the observed potentials are emphasized here, rather than the environments that caused the charging. Three events are shown, first the −19-kV eclipse event, then a −2-kV sunlight event. The latter event is compared with a −1.5-kV event previously published as a worst-case charging environment. The main purpose of showing the third event is to correct the earlier misidentification of that period as the −2-kV event. We begin with a brief description of the spacecraft and particle detectors, and then show the particle data from eclipse and sunlight.

Received May 31, 1985; revision received May 28, 1986.

*Assistant Research Professor, Physics Department; currently Associate Professor, Physics Department, Naval Postgraduate School, Monterey, CA.

Spacecraft and Detectors

The data in this paper come from the University of California at San Diego (UCSD) Auroral Particles Experiment on ATS-6 launched in May 1974. This was a three-axis-stabilized satellite in a geosynchronous orbit. The UCSD detector on ATS-6 detector was composed of five sets of electrostatic analyzers (ESAs), two for electrons, and three for ions. Paired ion and electron detectors were mounted in rotating assemblies, one rotating in the north-south plane (NS detector), the other in the east-west plane (EW detector). The third ion detector was fixed looking east. These detectors nominally measured 1-eV to 81-keV particles in 64 steps in 16 s.[10]

After 40 days of successful operation, the EW head suffered a partial failure in a high-voltage power supply, altering the energy coverage of the detector, in particular causing the low-energy data to be unreliable. Cross-talk between the ion and electron channels also increased. At about the same time, the fixed detector failed. These events limit the information which can be obtained during the record eclipse event, presented next.

Eclipse: The Record Potential

We begin by presenting the most negative potential measurement from the ATS-6 data set. This observation was made on October 8, 1975. A portion of these data has been presented in a review of charging.[11] Figure 1 is a spectrogram presentation of the particle fluxes as a function of time from the NS detectors.[1] Two hours of data are given in Fig. 1, with electron count rates in the top panel, and ion count rates in the bottom half. Both energy scales begin in the center, increasing up and down, respectively. High fluxes are plotted as white, low fluxes as dark gray or black. The gray scale has an overflow provision, where extremely high fluxes are plotted as black. This can be seen in the 10-keV ion data from 2145 to 2155 universal time (UT).

The eclipse period, as determined from the solar array telemetry, was from 2100 to 2155 UT. An injection of hot plasma, visible in the electron data at 2055 UT provides high fluxes of electrons at energies up to 80 keV. This causes the beginning of some differential and mainframe charging, and the spacecraft then abruptly drops to −6 kV at eclipse entry. The potential rises slowly to about −4 kV over the next 10 min. These potentials are revealed by the absence of ions below the potential energy attained by the ions falling onto the spacecraft, and then high fluxes at the spacecraft potential. There is some evidence for differential charging in the eclipse in the faintly visible trace of 100–200 eV electrons, most clearly visible at 2110 UT in the spectrogram. There is a drop in the flux of high-energy (1–20 keV) electrons beginning at 2112 which coincides with a drop in potential to below −10 kV between 2113 and 2120 UT. There are gaps in the data, but there is a clear measurement at −7 kV at 21:12:48 UT, with the potential apparently dropping below −10 kV in the next

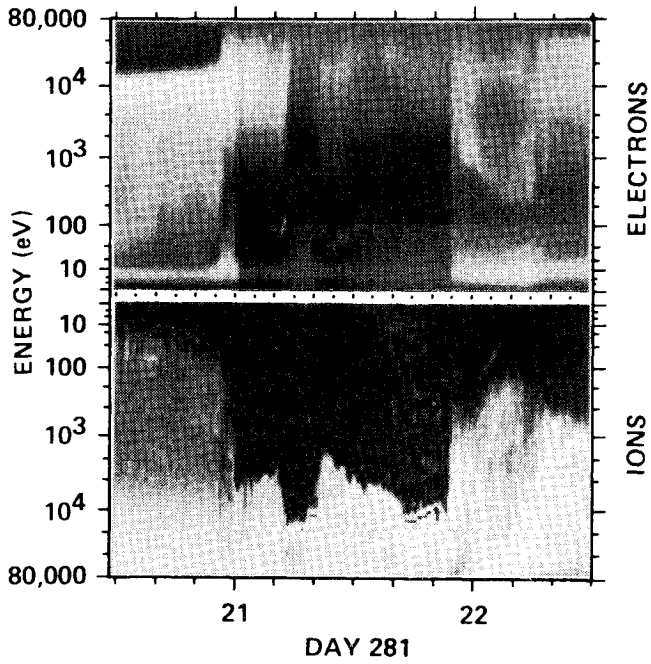

Fig. 1 Record eclipse charging event, October 8, 1975.

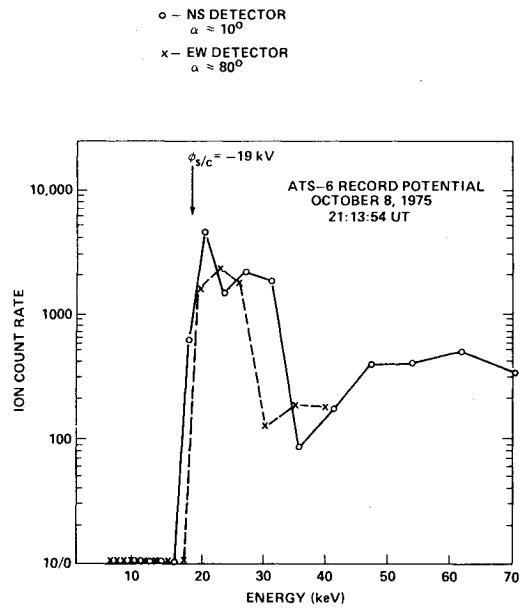

Fig. 2 Ion count rate, record charging event.

minute. The record measurement is found at 21:13:54 UT, as shown in Fig. 2. As also seen in the spectrogram, the ion count rate is zero at kinetic energies below the satellite potential. Ions accelerated from the distant, ambient plasma reach the detector at energies equal to and greater than 19 keV. The NS and EW detector agree on the −19-kV measurement. This is significant because the NS detector is measuring ions parallel to the magnetic field line ($\alpha \sim 10°$), while the EW detector is mesuring ions moving perpendicular to the magnetic field ($\alpha \sim 80°$). The potential rose to −16 kV at the next measurement at 21:14:25, and remained near that value till 21:19:12, when it rose to −11 kV. The potential wanders somewhat for the remainder of the eclipse, rising to about −100 V at eclipse exit. The last measurement is indistinct because of the lack of low-energy ion fluxes. The electron data (only shown in spectrogram form) provide a partial measure of the electron fluxes that cause the charging. The NS electron data show the field aligned fluxes between 12 and 71 keV are roughly Maxwellian, with a temperature of 17.7 keV, and a density of 0.29 cm^{-3}. The perpendicular electron data from the EW detector are contaminated by cross-talk. This is unfortunate, since these latter electrons probably provide the bulk of the charging current.

We conclude this set of observations by noting that K_p was 5 and 7 for the 3-h periods around 21 UT, and ΣK_p was 38 for the day. High magnetic activity has traditionally been associated with charging,[5] and these values support such an association.

Sunlight: −2 kV

The record daylight charging event occurred on August 5, 1974. The spacecraft charged to −2 kV, the most negative potential yet observed on any satellite in sunlight. Figure 3 is a spectrogram for 4 h of data, showing the local dawn charging period. (The satellite was stationed at −94°W, so local time (LT) is equal to UT −6.3 h.) The NS detector is looking along the magnetic field line ($\alpha \sim 10°$). The satellite is at low potential (~ -10 V) at 10 UT, then charges to −2000 V over the next 2 h, as shown by the ion data in Fig. 3. The −2-kV point

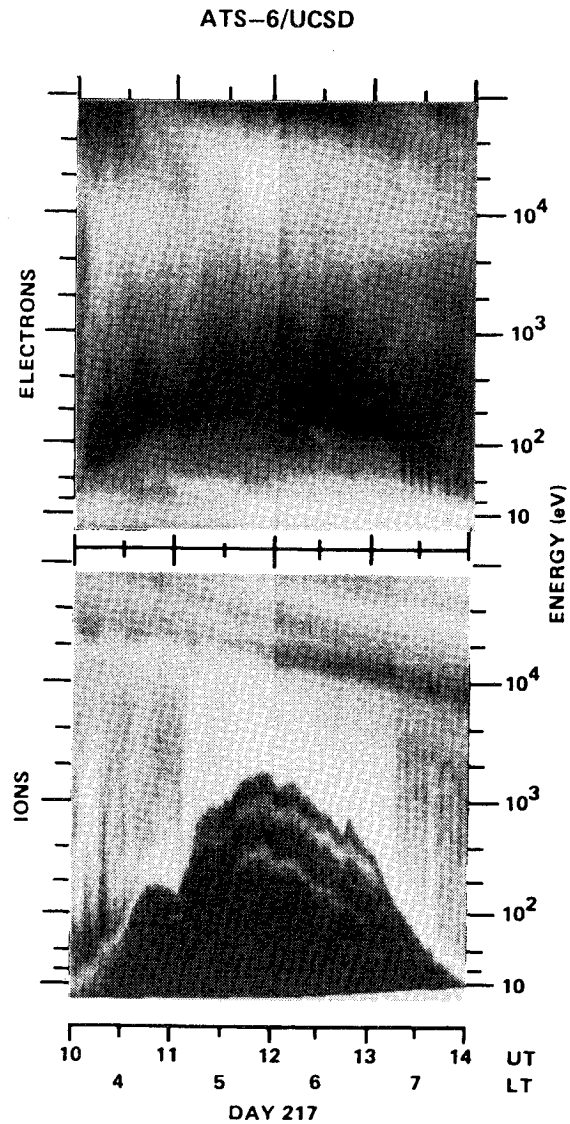

Fig. 3 Record daylight charging event, August 5, 1974.

is reached at 1155 UT. Following this, there is a nearly monotonic decline in potential as the plasma (electron) temperature drops. Figure 4 shows the electron and ion count rates at 1155 UT. The ion count rate shows a transition from near zero count rate to high count rate at 2 keV in both the perpendicular (EW) and field-aligned (NS) ions. Lower fluxes (10–30 counts/s) below 1 keV are attributed to ions generated on or near the spacecraft surface, which then return to the spacecraft.[7] The electron flux shows a peak at 18 keV, and high count rates below a few hundred electron-volts. The electrons measured below 250 eV are attributed to locally generated photoelectrons and secondary electrons, returned to the spacecraft by an electrostatic barrier. This barrier is the result of differential charging of insulating surfaces near the detector.[7]

Figure 5 shows the spacecraft potential over the record period, as determined from the peak in the ion count rate. Also plotted is the 18.2-keV electron count rate. Electron fluxes in this energy range have been shown to be crucial for the occurrence of charging at geosynchronous altitudes.[8,12] It can be seen that this was a long-lived event centered at local dawn, and that the variations in potential are rougly correlated with variations in the 18-keV electron flux.

The ion and electron distribution functions for the field-aligned particles measured by the NS detector are shown in Figs. 6 and 7, respectively. The distribution function, or phase space density, characterizes the particle distribution as a function of energy. Magnetospheric plasma, particularly electrons, can often be described as Maxwellian distributions (i.e., ther-

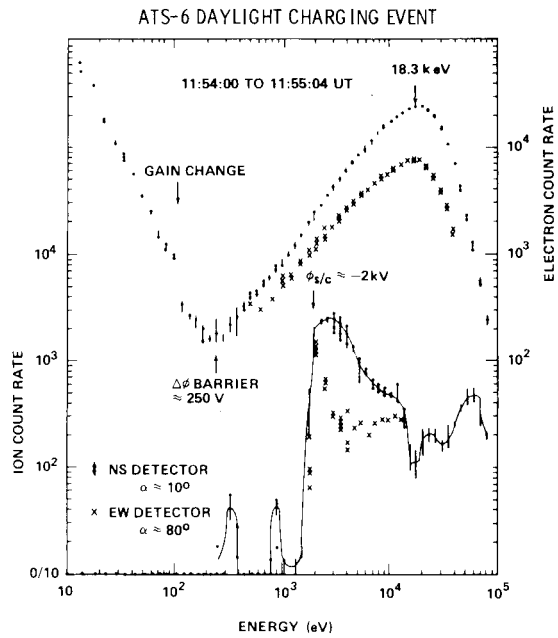

Fig. 4 Electron and ion count rate, August 5, 1974.

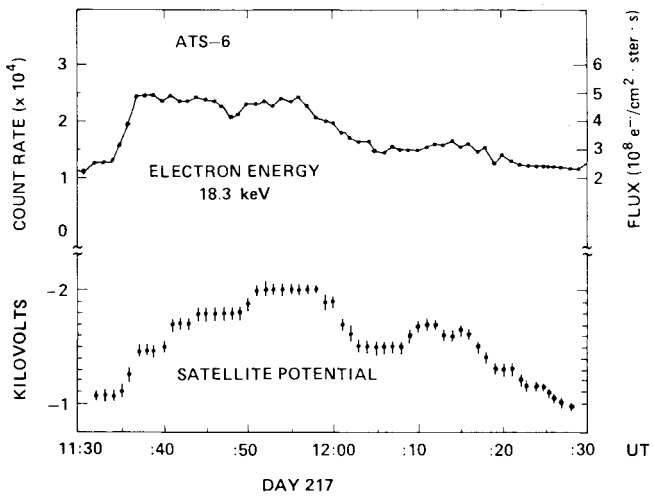

Fig. 5 Electron flux and satellite potential, August 5, 1974.

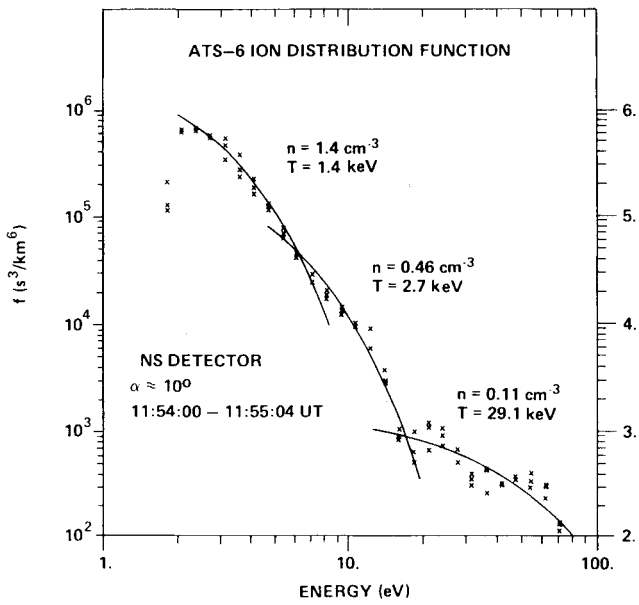

Fig. 6 Ion distribution function, August 5, 1974.

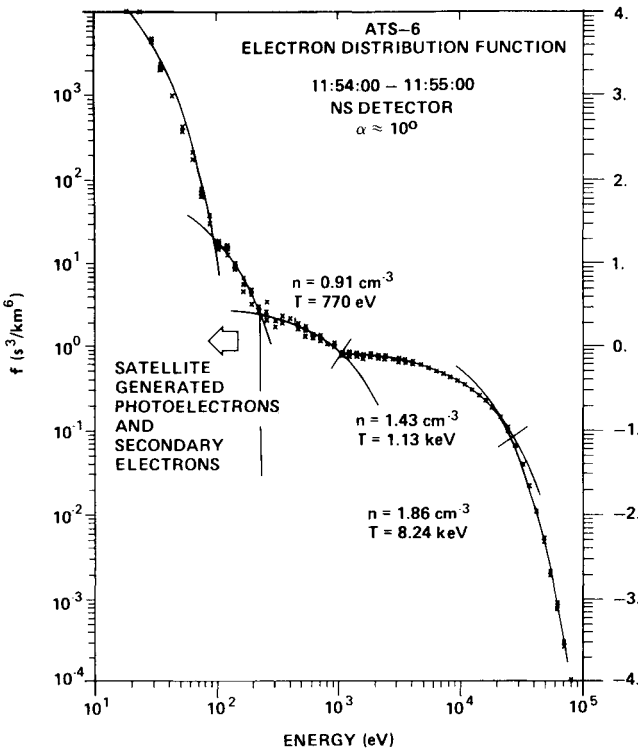

Fig. 7 Electron distribution function, August 5, 1974.

Table 1 Plasma parameters

	Energy range, eV[a]	Temperature, eV	Density, cm^{-3}[a]
	Day 217		
Electrons	2,250–3,050	770	0.91
	3,600–26,100	11,277	1.43
	29,600–83,500	8,244	1.86
Ions	750–5,100	1,391	0.77
	6,100–14,000	2,738	0.46
	16,400–79,500	29,082	0.11
	Day 178		
Electrons	2,000–2,500	558	1.07
	3,300–19,900	9,120	0.93
	22,500–83,000	19,700	0.96
Ions	600–22,600	6,469	0.14
	26,000–80,000	72,160	0.32

[a]Corrected for satellite potential.

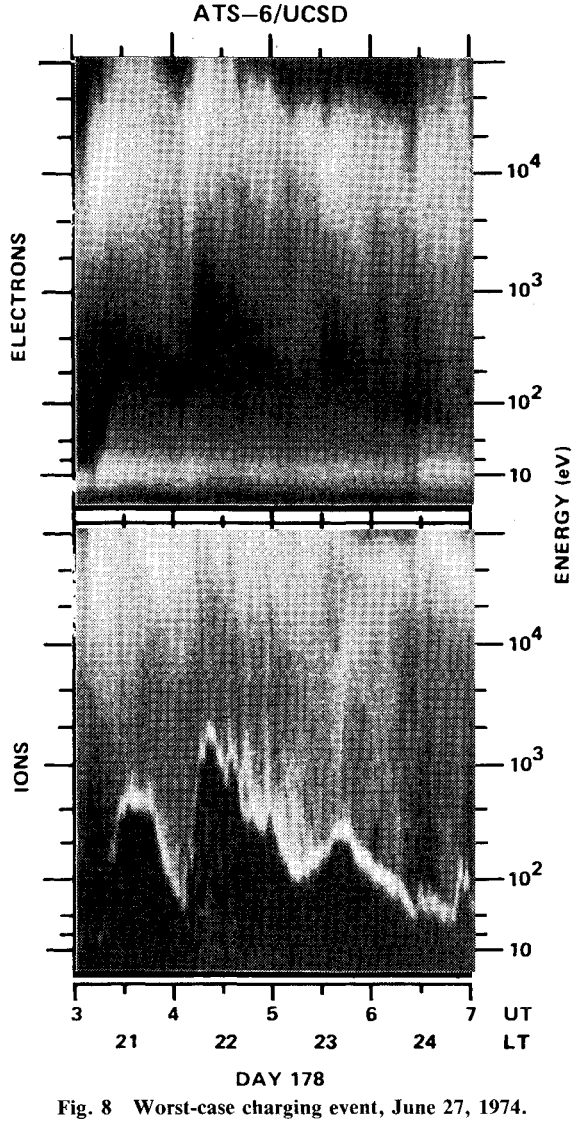

Fig. 8 Worst-case charging event, June 27, 1974.

malized distributions) over modest energy ranges. Such distributions can be recognized as straight line segments in plots of $\log f$ vs E. Piecewise least-square-fits have been made in order to characterize the plasma distributions for the use of those needing worst-case environments for charging studies.[8] The energy ranges, density, and temperature are given in Table 1. The ion distribution function has a temperature of

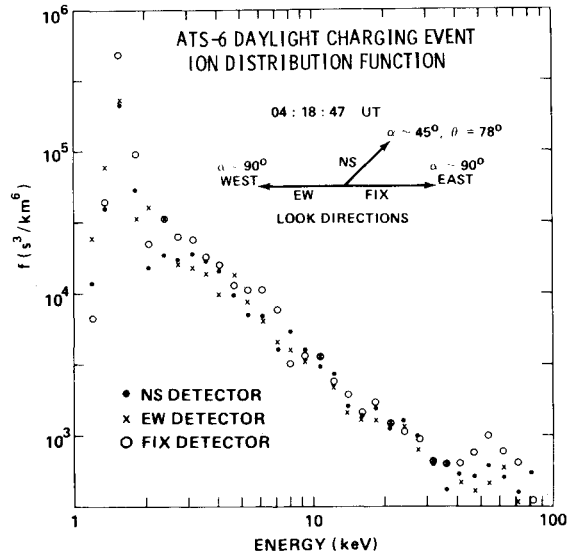

Fig. 9 Ion distribution function, June 27, 1974.

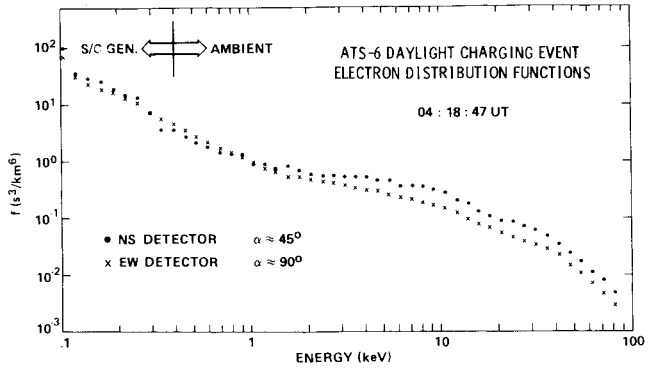

Fig. 10 Electron distribution function, June 27, 1974.

1.4 keV over the 0–8-keV energy range, while the electron distribution function is dominated by a 11.3-keV temperature between 1 and 25 keV. The data from the EW detector show the perpendicular electrons have similar characteristics. The electrons above 25 keV must be the remnant of a slightly earlier injection.[13]

Magnetic activity would be a relatively poor predictor for this day, since the 3-h K_p was only 3^+ during this event. Contrary to possible expectations, the record event did not occur at a time of very high magnetic activity.

Sunlight: −1.5 kV

A previously published example of daylight charging in ATS-6, on June 27, 1974, has been offered as an example of a worst-case environment.[9] Unfortunately, these data were presented as the −2kV event. In order to correct this error (which does not detract from the usefulness of the earlier work for use as a worst-case environment), the data are shown again here, and it is shown that the satellite potential for the June 27 charging event is −1.5 kV. Figure 8 shows 4 h of data around the premidnight event. The ion data show that the satellite is uncharged ($|\phi| < 10$V) at 0300 UT, charges to ~ −400 V at 0330, discharges, then charges again from 0400 to 0418 UT, reaching −1500 V at 0418. The satellite discharges again between 0418 and 0500 as the ambient electron energy decreases. Ion and electron distribution functions taken at 0419 UT on June 27, 1974 (day 178) are shown in Figs. 9 and 10. Figure 9

shows that the ion distribution function peaks at 1.5 keV, indicating a satellite potential of −1.5 kV. The three-ion detectors give similar measurements, indicating that the ion distribution is not highly anisotropic at the observed pitch angles. (Note, however, that the minimum pitch angle measured here is 45 deg.) The ion data in Fig. 9, and the electron data shown in Fig. 10 were fitted with Maxwellian segments, with results given in Table 1. Electron data below 400 eV were excluded because of differential charging effects. The ion distribution function flattens above 24 keV, and is characterized by a temperature over 50 keV. Aside from the minor correction introduced by the different satellite potential used here, the numbers presented in Table 1 are equivalent to those presented previously.[9] The discrepancy in ion and electron densities partially reflects the lack of information on ion composition. If the ambient ions are mostly oxygen, which can be true during magnetically active times, then the value for the ion density inferred from the electrostatic analyzer can be low by as much as a factor of 4. Also, the inner plasma sheet is typically dominated by magnetic field-aligned ions, which are not well sampled at this time by the UCSD detector.[14,15] By comparison with the previous event (day 217), the electron temperature is higher for this event and hence this event still provides a better environment for charging predictions. The difference in the measured potentials reflects the importance of the time history of the environment.

Summary

The record eclipse and daylight charging events shown here for ATS-6 establish the magnitude of satellite potentials that can be encountered at geosynchronous orbit. Differential charging (of insulated surfaces) of similar magnitudes is clearly possible, though details of satellite geometry, local fields, and surface conductivity effects may limit the surface potentials attained before arcing occurs. The fact that the record daylight event occurred at local dawn suggests that the −20-kV potential found in eclipse at local midnight could be exceeded by shadowed surfaces on any geosynchronous satellite. This is a strong argument for not allowing permanently shadowed ends of spinning spacecraft to have insulating surfaces, since differential potentials of kilovolts can easily be developed. Electrostatic cleanliness is essential, not only for scientific measurements, but for spacecraft safety. One alternative to conducting surfaces is to provide an active means of charge control, such as a plasma source.[16]

Acknowledgments

The data reported in this paper were provided by Dr. C. E. McIlwain, the principal investigator for the UCSD instrument. The analysis was funded by NASA/MSFC under contract NAS8-33982 and NASA/LeRC under contract NAG3-620.

References

[1]DeForest, S. E., "Spacecraft Charging at Synchronous Orbit," *Journal of Geophysical Research,* Vol. 77, 1972, pp. 651–659.

[2]DeForest, S. E., "Electrostatic Potentials Developed by ATS5," in *Photon and Particle Interactions with Surfaces in Space*, edited by R.J.L. Grard, D. Reidel, Hingham, MA, 1973, pp. 263–276.

[3]Olsen, R. C. and Purvis, C. K., "Observations of Charging Dynamics," *Journal of Geophysical Research*, Vol. 88, 1983, pp. 5657–5667.

[4]Garrett, H. B. and DeForest, S. E., "Time-varying Photoelectron Flux Effects on Spacecraft Potential at Geosynchronous Orbit," *Journal of Geophysical Research*, Vol. 84, 1979, pp. 2083–2088.

[5]Garrett, H. B., "The Charging of Spacecraft Surfaces," *Review of Geophysics and Space Physics*, Vol. 19, 1981, pp. 577–616.

[6]Reasoner, D. L., Lennartsson, W., and Chappell, C. R., "Relationship Between ATS6 Spacecraft-Charging Occurrences and Warm Plasma Encounters," in *Spacecraft Charging by Magnetospheric Plasmas, Progress in Astronautics and Aeronautics*, Vol. 47, edited by A. Rosen, AIAA, New York, 1976, pp. 89–101.

[7]Olsen, R. C., McIlwain, C. E., and Whipple, E. C., "Observations of Differential Charging Effects on ATS6," *Journal of Geophysical Research*, Vol. 86, 1981, pp. 6809–6819.

[8]Gussenhoven, M. S. and Mullen, E. G., "Geosynchronous Environment for Severe Spacecraft Charging," *Journal of Spacecraft and Rockets*, Vol. 20, Jan.–Feb. 1983, pp. 26–34.

[9]Deutsch, M.-J. C., "Worst Case Charging Environment," *Journal of Spacecraft and Rockets*, Vol. 19, Sept.–Oct. 1982, pp. 473–477.

[10]Mauk, B. H. and McIlwain, C. E., "ATS6 UCSD Auroral Particles Experiment," *ISEE Transactions on Aerospace and Electronic Systems,* Vol. AES-11, 1975, pp. 1125–1130.

[11]Whipple, E. C., Jr., "Potentials of Surfaces in Space," *Reports on Progress in Physics*, Vol. 44, 1981, pp. 1197–1250.

[12]Olsen, R. C., "A Threshold Effect for Spacecraft Charging," *Journal of Geophysical Research*, Vol. 88, 1983, pp. 493–499.

[13]DeForest, S. E. and McIlwain, C. E., "Plasma Clouds in the Magnetosphere," *Journal of Geophysical Research*, Vol. 76, 1971, pp. 3587–3611.

[14]Olsen, R. C., "Field Aligned Ion Streams in the Earth's Midnight Region," *Journal of Geophysical Research*, Vol. 87, 1982, pp. 2301–2310.

[15]Lennartsson, W. and Sharp, R. D., "A Comparison of the 0.1–17 keV/e Ion Composition in the Near Equatorial Magnetosphere Between Quiet and Disturbed Conditions," *Journal of Geophysical Research*, Vol. 87, 1982, pp. 6109–6120.

[16]Olsen, R. C., "Modification of Spacecraft Potentials by Plasma Emission," *Spacecraft and Rockets,* Vol. 18, Sept.–Oct. 1981, pp. 462–469.